

# Seismic stratigraphy interpretation by deep convolutional neural networks: A semisupervised workflow

Haibin Di<sup>1</sup>, Zhun Li<sup>1</sup>, Hiren Maniar<sup>1</sup>, and Aria Abubakar<sup>1</sup>

## ABSTRACT

Depicting geologic sequences from 3D seismic surveying is of significant value to subsurface reservoir exploration, but it is usually time- and labor-intensive for manual interpretation by experienced seismic interpreters. We have developed a semisupervised workflow for efficient seismic stratigraphy interpretation by using the state-of-the-art deep convolutional neural networks (CNNs). Specifically, the workflow consists of two components: (1) seismic feature self-learning (SFSL) and (2) stratigraphy model building (SMB), each of which is formulated as a deep CNN. Whereas the SMB is supervised by knowledge from domain experts and the associated CNN uses a similar network architecture typically used in image segmentation, the SFSL is designed as an unsupervised process and thus can be performed backstage while an expert prepares the training labels for the

SMB CNN. Compared with conventional approaches, the our workflow is superior in two aspects. First, the SMB CNN, initialized by the SFSL CNN, successfully inherits the prior knowledge of the seismic features in the target seismic data. Therefore, it becomes feasible for completing the supervised training of the SMB CNN more efficiently using only a small amount of training data, for example, less than 0.1% of the available seismic data as demonstrated in this paper. Second, for the convenience of seismic experts in translating their domain knowledge into training labels, our workflow is designed to be applicable to three scenarios, trace-wise, paintbrushing, and full-sectional annotation. The performance of the new workflow is well-verified through application to three real seismic data sets. We conclude that the new workflow is not only capable of providing robust stratigraphy interpretation for a given seismic volume, but it also holds great potential for other problems in seismic data analysis.

## INTRODUCTION

Seismic stratigraphy interpretation aims at depicting subsurface geologic sequences from 3D seismic surveys, and accurate stratigraphic delineation has wide applications in robust reservoir exploration. To achieve such a goal, conventional workflows often integrate horizon tracking and geologic modeling. Specifically, in the horizon tracking step, a seismic interpreter picks a set of seismic reflectors, each of which represents one of the important geologic boundaries, whereas the geologic modeling step provides a mathematical solution for stacking the picked seismic horizons in 3D space and reconstructing the sequence model by following the fundamental geologic rules (e.g., no horizon crossing). Apparently, the accuracy of the built seismic stratigraphy is most likely determined by the accuracy of horizon tracking. Previous efforts have been

devoted to this topic (e.g., Harrigan et al., 1992; Leggett et al., 1996; Huang, 1997; Hoecker and Fehmers, 2003; Farakliti and Petrou, 2004; Patel et al. 2010; Yu et al., 2008, 2011; Herron, 2011, 2015; Gramstad and Bakke, 2012; Wu and Hale, 2015), such as seeded autotracking based on the lateral continuity of seismic signals such as amplitude and gradient. It is well-tested that the performance of such automatic horizon tracking greatly depends on the quality of seismic horizons, which works effectively for reflections with a strong amplitude, high signal-to-noise ratio (S/N), and high degree of lateral continuity (Herron, 2015). However, in most cases, the subsurface structures are of high complexities; correspondingly, the horizons in a 3D seismic data set are often of a low amplitude, low S/N, and/or low degree of lateral continuity. When performed on such a low-quality horizon, the conventional horizon tracker is highly prone to two types of problems (Di et al. 2018a). First, the tracked horizon is piloted by the nearly strong

Manuscript received by the Editor 16 July 2019; revised manuscript received 16 January 2020; published ahead of production 16 March 2020; published online 30 April 2020.

<sup>1</sup>Schlumberger, Exploration and Field Development Platform, Data Analytics Program, Houston, Texas 77042, USA. E-mail: hdi@slb.com (corresponding author); zli68@slb.com; hmaniar@slb.com; aabubakar@slb.com.

© 2020 Society of Exploration Geophysicists. All rights reserved.

reflection, causing the tracked horizon to deviate from the right track of the intended one. Second, the tracking terminates unexpectedly at local discontinuities, where the reflection is either poorly imaged or significantly changed, causing the reflection continuity to fall below the confidence level for the tracking to continue.

The recent success of machine learning, particularly the convolutional neural network (CNN) in image processing (e.g., Zeiler et al., 2011; Long et al., 2015; Ronneberger et al., 2015; Kallenberg et al., 2016; Badrinarayanan et al., 2017) has brought new insights and tools into the vision of seismic interpreters, and enormous efforts have been made in efficiently using deep CNNs for resolving the typical problems in seismic pattern recognition and interpretation, such as saltbody delineation and fault detection (e.g., Araya-Polo et al., 2017; Huang et al., 2017; AlRegib et al., 2018; Di et al., 2018b, 2018c, 2019a; Guitton, 2018; Wang et al., 2018; Xiong et al., 2018; Zhao and Mukhopadhyay, 2018; Wu et al., 2019a; Di and AlRegib, 2020). On the contrary, only a little research has been done toward CNN-assisted seismic stratigraphy interpretation (e.g., Di et al., 2019b, 2019c; Geng et al., 2019; Li et al., 2019; Peters et al., 2019; Wu et al., 2019b). For

example, Geng et al. (2019) present a CNN for estimating the relative geologic time; Wu et al. (2019b) apply the encoder-decoder CNNs for seismic horizon interpretation; and Peters et al. (2019) investigate the feasibility of seismic horizon tracking from few training images.

It appears straightforward for extending the CNNs from fault/salt to stratigraphy; however, we notice two major limitations. First, a large amount of training data is often required to build a reliable interpretation machine, which are either not readily available in or require lots of effort from an experienced seismic interpreter for preparing them. Otherwise, overfitting would occur, which restricts the CNN performance on the training data only. Second and more importantly, applying convolutional CNNs typically requires the training seismic sections to be fully labeled, which is not always feasible in annotating seismic data, due to not only the intensive labor for full-sectional seismic annotation, but also the interpretational uncertainties existing in seismic sections of subsurface complexities.

To address both limitations, this study presents a semisupervised workflow for automatic seismic stratigraphy interpretation through deep CNNs, which consists of two steps: (1) seismic feature self-learning (SFSL) and (2) stratigraphic model building (SMB).

In this paper, we will first describe the two-step workflow. Then, we propose three use cases for applying the proposed workflow in practice. Next, the proposed workflow is verified through application to multiple real 3D seismic surveys. Finally, we quality check the results and compare the performance of the proposed workflow with conventional approaches.

## PROPOSED WORKFLOW

Figure 1 illustrates the proposed workflow for seismic stratigraphy interpretation via deep CNNs, which is semisupervised and consists of two steps: SFSL and SMB. Specifically, given a seismic data set, the step of SFSL aims at understanding the features in the seismic data set by a deep CNN itself, which is purely unsupervised and requires no input from seismic interpreters. Then, in the SMB step, a second deep CNN is built on the SFSL CNN for learning and recognizing the target seismic stratigraphic sequences, which is guided by knowledge from an expert to ensure the machine prediction reliable in geology. In the section below, we describe each step in detail.

### SFSL

The goal of the SFSL is to build a deep CNN capable of parsing and understanding the seismic features by itself, so that its knowledge can be inherited while building and training the SMB CNN. The benefits of building the SFSL CNN are two-fold: (1) faster model training with lower initial loss and (2) better generalization ability for long-distance prediction, as is exclusively illustrated in the “Results” section.

To avoid introducing bias from seismic interpreters, we propose accomplishing the SFSL without requiring any domain knowledge, which

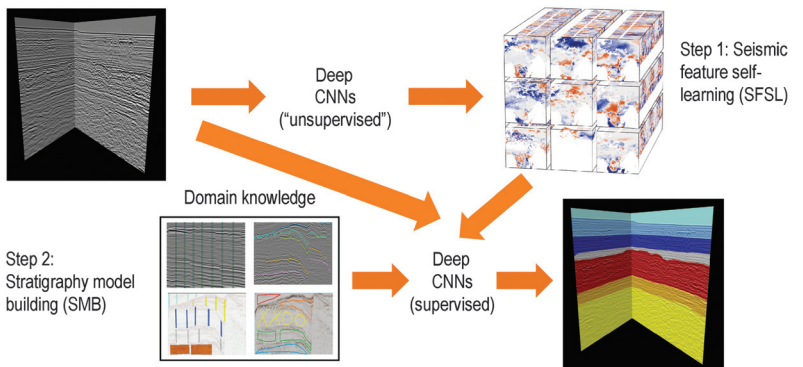


Figure 1. The proposed semisupervised workflow of seismic stratigraphy interpretation through deep CNNs, which consists of two components: (a) SFSL and (b) SMB.

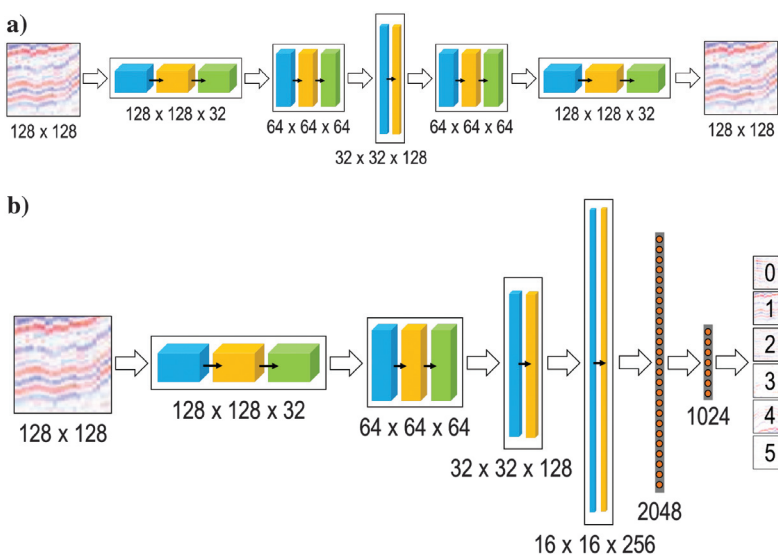


Figure 2. The architectures for two CNNs for the SFSL proposed in this work: (a) the convolutional autoencoder and (b) the six-rotation classifier.

can be achieved in two ways. The most straightforward approach is to use a convolutional autoencoder, which aims at reconstructing the seismic signals through an encoder-decoder architecture (Figure 2a). Specifically, the encoder, when treated as a feature extractor, generates a large set of intermediate features from the input seismic amplitude, whereas the decoder aims at integrating these features back to the original amplitude with minimum difference.

Whereas the autoencoder network learns seismic features by maximally reconstructing the seismic amplitude, an alternative approach is to deliberately edit the seismic signal and build a CNN for identifying how the signal has been edited, such as geometric transformations (Agrawal et al., 2015; Dosovitskiy et al., 2016; Gidaris et al., 2018). One example of such seismic signal editing is to first cut a seismic volume into a set of tiles and then rotate each of the tiles in six ways, including  $0^\circ$ -,  $90^\circ$ -,  $180^\circ$ -, and  $270^\circ$ -rotation and left-right and up-down transposition. The corresponding CNN is then designed as a six-rotation classifier, which typically consists of a set of convolutional layers followed by a set of fully connected layers and determines how a tile of seismic signal is rotated (Figure 2b). Specifically, in such an architecture the seismic features are learned and extracted by the convolutional layers, whereas the fully connected layers connect the mapping relationship between the extracted features and the six types of rotation.

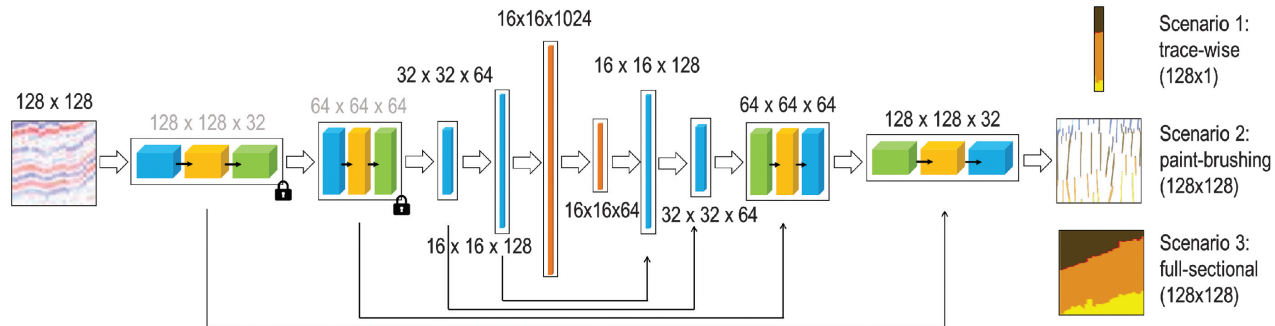


Figure 3. The architectures of three CNNs for the SMB proposed in this work, each of which corresponds to one application scenario illustrated in Figure 4.

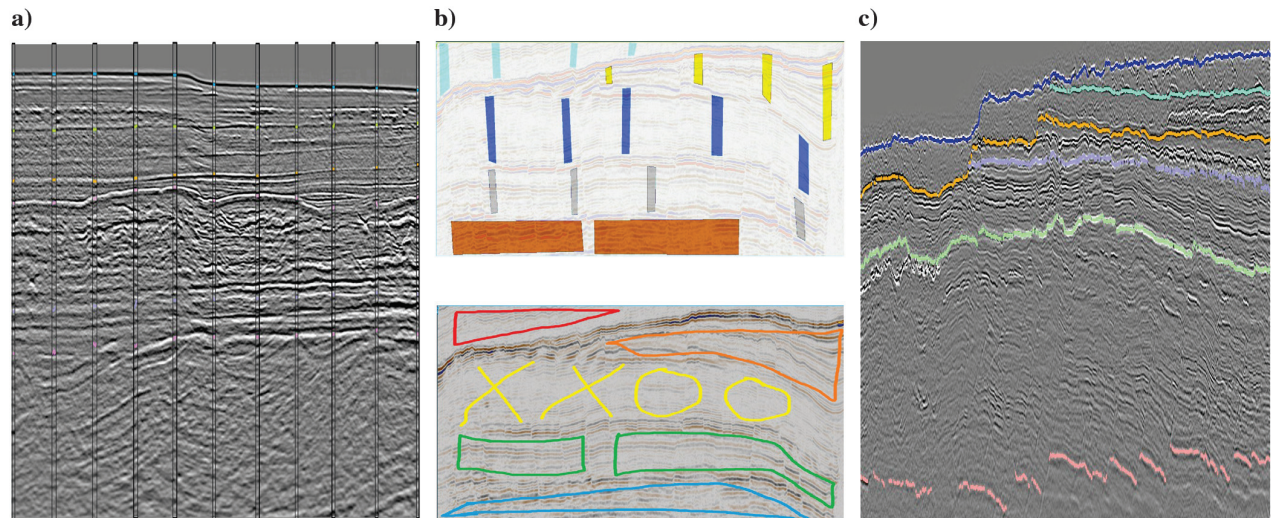


Figure 4. The three scenarios for applying the proposed seismic stratigraphy interpretation, in which the expert annotations can be provided at trace-wise (a), paintbrushing (b), and full-sectional (c), respectively. The corresponding three SMB CNNs are illustrated in Figure 3.

## SMB

In the SMB step, we build a machine capable of mimicking an interpreter's intelligence and recognizing the target seismic sequences. We design such a machine in the typical architecture of a fully convolutional neural network (Noh et al., 2015; Ronneberger et al., 2015; Badrinarayanan et al., 2017). In general, given a seismic image, the SMB CNN first extracts a set of features from it and then predicts the corresponding stratigraphic sequences from the extracted features. As illustrated in Figure 3, this study builds the SMB CNN from the pretrained SFSL CNN instead of from scratch. Therefore, the feature extraction is locked and will not be modified during SMB training. With the SFSL CNN well trained, the locked feature extraction forces the SMB CNN to use the general features in the entire seismic volume while building the mapping relationship, so that it would be applicable not only to the training data but also to the rest of the data in the target seismic data set.

In this study, we present three architectures for the SMB CNN (Figure 3), each of which corresponds to one of the three scenarios as described in the next section for applying the proposed seismic stratigraphy interpretation in practice (Figure 4).

## APPLICATION SCENARIOS

For the convenience of seismic interpreters providing their knowledge for training the SMB CNN in an efficient way, we identify three application scenarios, in which the expert annotation is of three different forms; correspondingly, the SMB CNN varies slightly in its architecture. As shown in Figure 4, the three application scenarios are:

- 1) **Trace-wise** annotation, in which an interpreter selects a few representative seismic traces and marks the target sequence boundaries. Then, given a seismic tile, the SMB CNN extracts all of the features in it but predicts the stratigraphic sequences only at the central trace.
- 2) **Paintbrushing** annotation, in which an interpreter uses a paintbrush to highlight the target seismic sequences. Correspondingly, given a seismic tile, the SMB CNN extracts all the features in it but predicts the stratigraphic sequences only in the zones of interest that the interpreter has specified.
- 3) **Full-sectional** annotation, in which a few seismic sections are fully interpreted. Based on that, given a seismic tile, the SMB

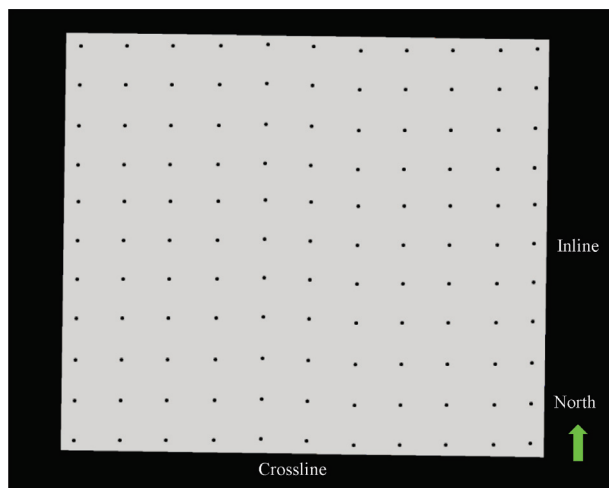


Figure 5. The map view of the Gullfaks seismic survey (denoted by the rectangle) and the annotated 121 traces (denoted by the dots) used for demonstrating the application of the proposed workflow in the trace-wise scenario.

Figure 6. An example of the trace-wise annotation in the inline 2650, in which the six important stratigraphic boundaries are marked in 11 traces.

CNN extracts all the features in it and predicts the stratigraphic sequences in the entire tile.

In comparing the three scenarios, the full-sectional scenario is the easiest for implementation from the perspective of machine learning algorithms but requires the most intensive interpreter labor for training data preparation and is thus of limited application in practice. On the contrary, the trace-wise scenario requires the least training data and moreover is integrable with well interpretation. The paintbrushing scenario is most flexible in terms of data preparation, in which an interpreter is capable of annotating any zones of interest in a seismic data set.

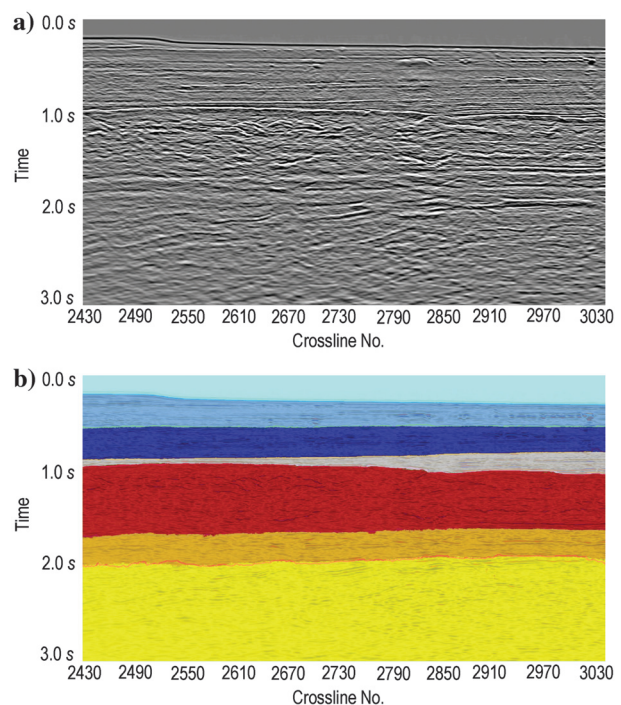
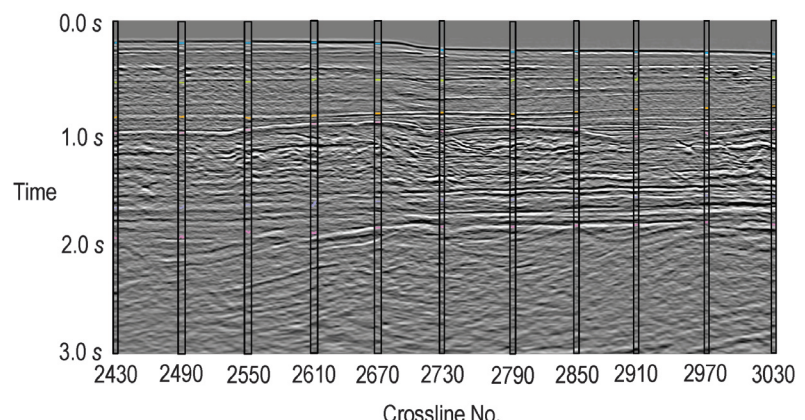


Figure 7. (a) The amplitude and (b) the six sequences predicted by the proposed trace-wise seismic stratigraphy interpretation in inline 2850. Colors are randomly assigned for the sole purpose of visualization. Note the successful tracking of the corresponding sequences through the entire section from the given 121 traces in Figure 6.



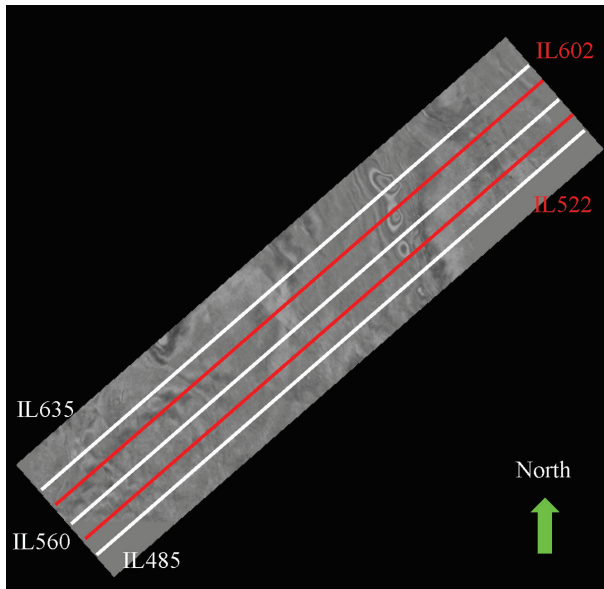


Figure 8. Map view of the North Sea seismic survey (denoted by the rectangle) and the five inline sections (denoted by the white lines) used for demonstrating the application of the proposed workflow in the paintbrushing scenario, including three training sections of paintbrushing annotations (IL485, IL560, and IL635) (denoted by the white lines) and two prediction sections (IL522 and IL602) (denoted by the red lines). The corresponding sequence interpretations are shown in Figures 9 and 10, respectively.

## RESULTS

After illustrating the proposed workflow, we then demonstrate its applications through three real examples, each corresponding to one of the three scenarios shown in Figure 4.

### Example 1: Trace-wise

In this example, we use a 3D seismic data set over the Gullfaks oil field in Norway, which covers an area of 47 km<sup>2</sup> and consists of 501 inlines, 601 crosslines, and 751 samples per trace. For applying the proposed workflow in the trace-wise scenario, 121 traces are selected and marked in a regular grid of 11 inlines by 11 crosslines, which is about 0.04% of the available seismic data. Figure 5 displays the map view of the seismic survey and the 121 marked seismic traces (denoted by black dots). As illustrated in Figure 4a, the trace-wise scenario requires no sequence annotation but only the boundaries, and Figure 6 displays an example of the trace-wise annotation in the vertical section of inline 2650, in which only 11 traces are marked. Six boundaries are of the interpretational interest in this example.

After applying the proposed workflow, a sequence cube is generated in the same size as the seismic survey. For the convenience of quality control, the amplitude and the corresponding sequence interpretation in the vertical section of inline 2850 are shown in Figure 7. It is clear that, with the 0.04% training data, the proposed workflow successfully extends the trace-wise annotations to the entire seismic volume and segments it into the seven target stratigraphic sequences, with the sequence boundaries matching well with the seismic

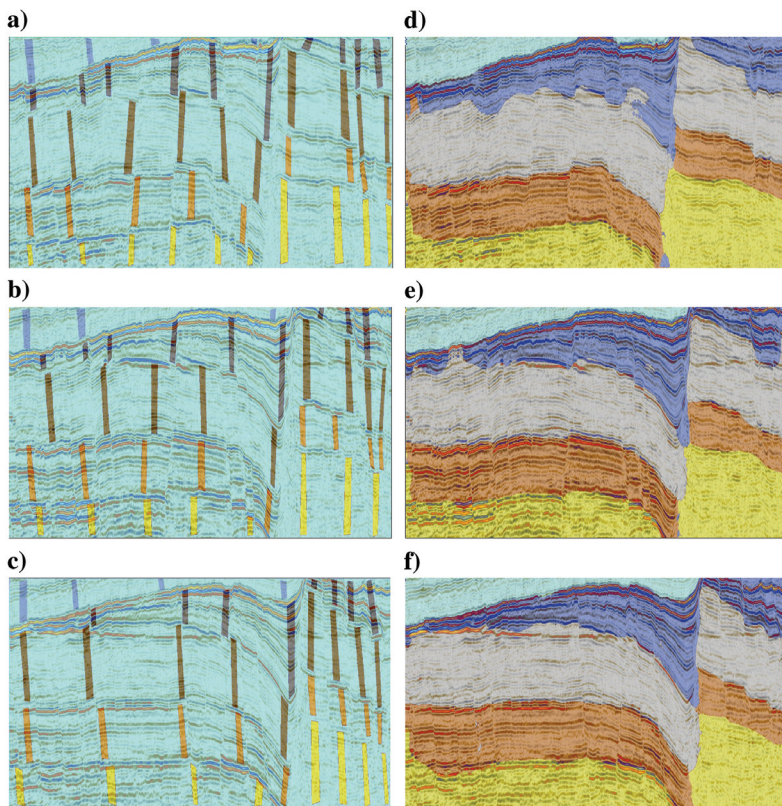


Figure 9. (a-c) The paintbrushing annotation and (d-f) the machine prediction (d-f) of the three training inline sections (IL485, IL560, and IL635).

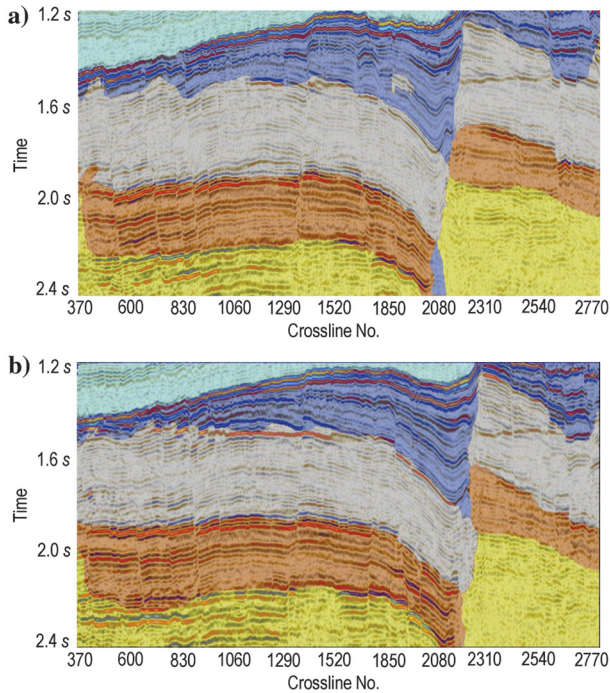


Figure 10. The seismic stratigraphy interpretation by the proposed workflow in the paintbrushing scenario in the two prediction inline sections (denoted by the red lines in Figure 8), including (a) inline 522 and (b) inline 602.

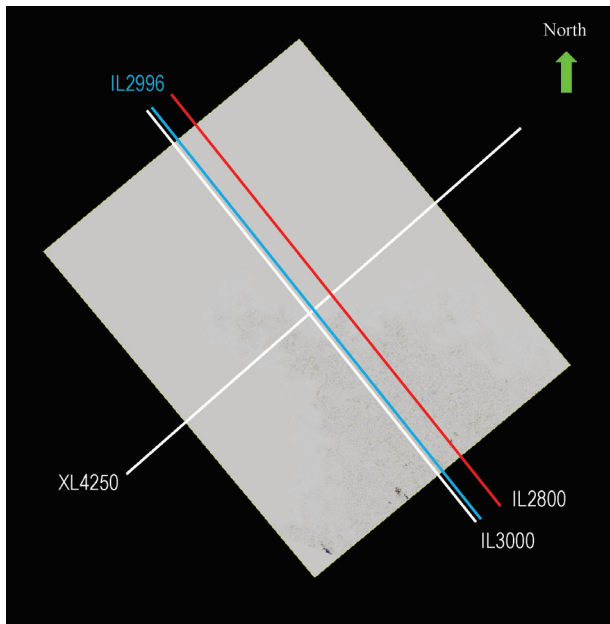


Figure 11. The map view of the Solsikke seismic survey (denoted by the rectangle) and the four sections used for demonstrating the application of the proposed workflow in the full-sectional scenario, including two training sections (IL3000 and XL4250) (denoted by the white lines), one testing section (IL2996) (denoted by the blue line), and one prediction section (IL2800) (denoted by the red line). The corresponding sequence interpretation is shown in Figures 13–15, respectively.

events. The color is randomly assigned for the sole purpose of visualization and has no geologic implications.

### Example 2: Paintbrushing

In this example, we use a subset of the NH seismic data set over the North Sea, which covers an area of 162 km<sup>2</sup> and consists of 333 inlines, 2176 crosslines, and 576 samples per trace. For applying the proposed workflow in the paintbrushing scenario, the sequences in three inline sections (IL485, IL560, and IL635; denoted by the white lines in Figure 8) are manually marked by a paintbrush, which is about 0.9% of the available seismic sections. As illustrated in Figure 4b, the paintbrushing scenario requires representative expert interpretation of the target sequences, and Figure 9a–9c displays the paintbrushing annotation in the three training sections (IL485, IL560, and IL635), in which five sequences are of interpretational interest. Note that in the paintbrushing scenario, an interpreter is allowed to conduct his annotation in any shape or orientation, such as the stripes used in this example. Because the three training sections are partially annotated, the training amount is estimated as 0.05% of the available seismic data. More importantly, such annotation does not necessarily touch the sequence boundaries, which makes it possible to avoid interpreter bias due to the interpretational uncertainties in the zones of low seismic quality.

After applying the proposed workflow, a sequence cube is generated in the same size as the NH seismic survey. For the convenience of quality control, the prediction is clipped to the three training sections (Figure 9d–9f) and the two prediction sections (Figure 10). The interpretation in this data is challenged by the major fault, which not only breaks the sequence continuity but also

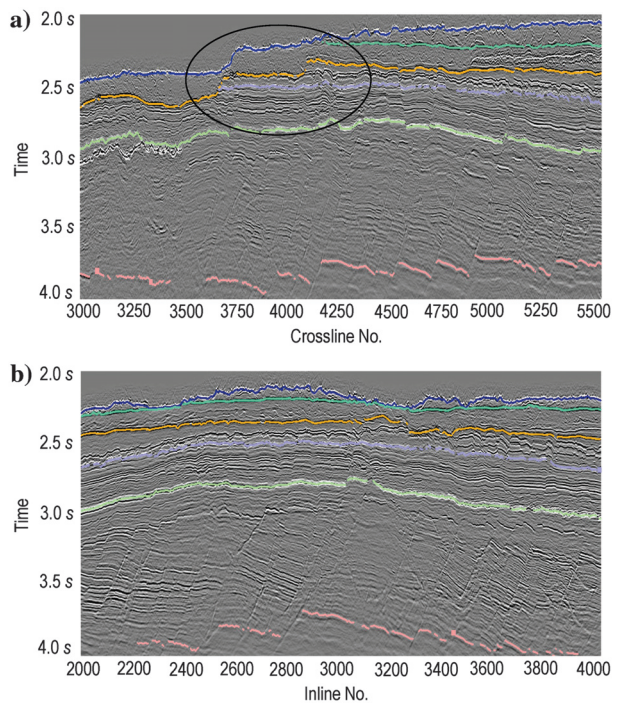


Figure 12. The full-sectional annotations in the two training sections, including (a) inline 3000 and (b) crossline 4250. Note the pinch-out structures (denoted by the circle) and the bad quality of the seismic signals in the bottom area.

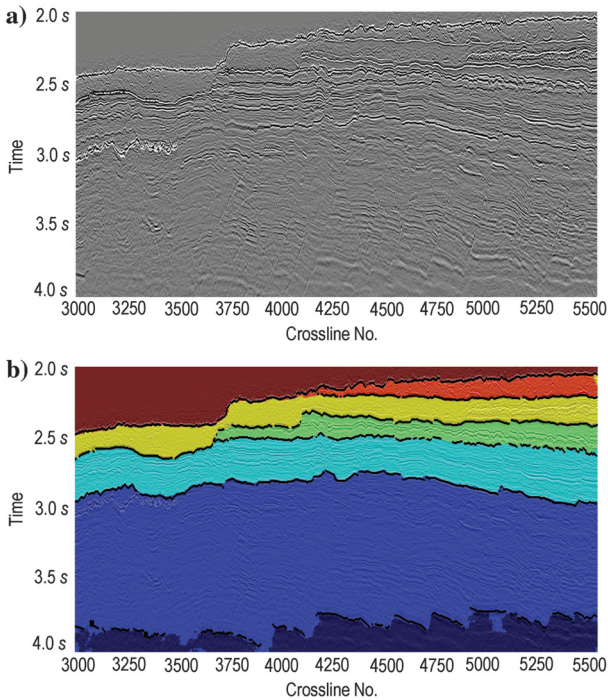


Figure 13. (a) The amplitude and (b) the sequence interpretation by the proposed workflow in the full-sectional scenario to the training section of inline 3000. The expert annotations are highlighted as the black curves.

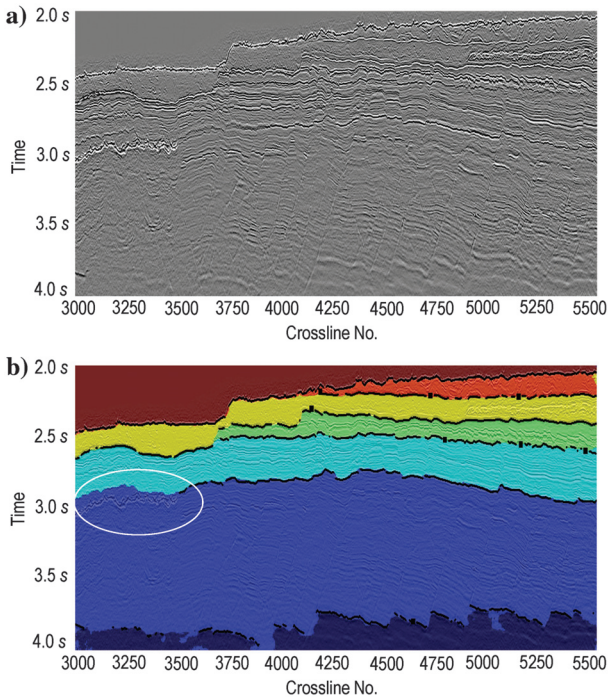


Figure 14. (a) The amplitude and (b) the sequence interpretation by the proposed workflow in the full-sectional scenario to the testing section of inline 2996. The expert annotations are highlighted as the black curves. Note the good match between the interpretation and the expert annotations as well as the successful tracking in the areas of no expert interpretation (denoted by the circle).

weakens the signal quality in the footwall block. However, given the 0.05% training data, the proposed workflow is capable of continuously tracking the sequences across the major fault. The misannotations near the fault are expected to be reduced/eliminated by feeding more expert knowledge. The color is randomly assigned for the sole purpose of visualization and has no geologic implications.

### Example 3: Full-sectional

In this example, we use a larger 3D seismic survey from Solsikke, which covers an area of 744 km<sup>2</sup> and consists of 996 inlines, 1251 crosslines, and 574 samples per trace. For applying the proposed workflow in the full-sectional scenario, the sequences in two sections, including inline 3000 and crossline 4250 (denoted by the white lines in Figure 8), which is about 0.08% of the available seismic data. Seven sequences are of interpretational interest in this example. In addition to the two training sections, expert annotations are also provided for inline 2996, which was not used for machine training but purely for testing the performance of the proposed workflow. Figure 11 shows the location of the four sections, including the two training sections (IL3000 and XL4250) (denoted by the white lines), one testing section (IL2996) (denoted by the blue line), and one prediction section (IL2800) (denoted by the red line). Figure 12 shows the manual annotation of the two training sections. The corresponding stratigraphy interpretation by the proposed workflow is shown in Figures 13, 14, and 15.

After applying the proposed workflow, a sequence cube is generated in the same size as the Solsikke seismic survey. For the convenience of quality control, the prediction is clipped to the training section (IL3000) (Figure 13), the testing section (IL2996) (Figure 14), and the prediction section (IL2800) (Figure 15). Given the 0.08% training data, the proposed workflow is capable of well tracking the

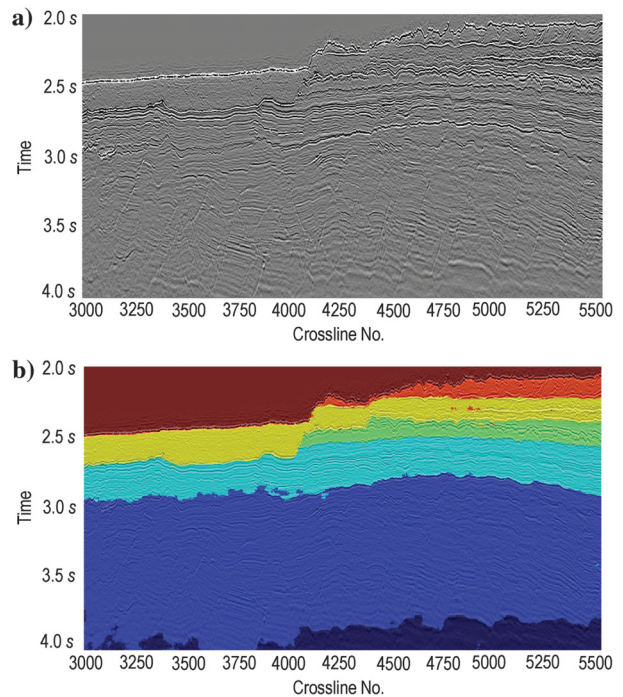


Figure 15. (a) The amplitude and (b) the sequence interpretation by the proposed workflow in the full-sectional scenario to the prediction section of inline 2800. Note the good match between the interpretation and the seismic amplitude.

sequences, particularly those in the shallow area of good seismic data quality. The accuracy in the bottom is expected to be further improved by exposing the machine with more data from the bottom area. The color is randomly assigned for the sole purpose of visualization and of no geologic implications.

Figure 16 displays the 3D view of three sequence boundaries (or horizons) generated from the machine prediction in the Solsikke data set, colored by depth (a-c) and amplitude (d-f), respectively, demonstrating the good spatial continuity and consistent seismic signature throughout these horizons from the proposed method. In addition, Figure 17 compares the seafloor, the top horizon in the Solsikke data set, extracted by the proposed method, and the conventional horizon tracker. Both extractions appear similar. It is expected that with the geologic complexity increasing from top to bottom in this area, picking the rest of the

Figure 16. A 3D view of three of the six horizons in the Solsikke data set extracted from the machine prediction, colored by (a-c) depth and (d-f) amplitude, respectively.

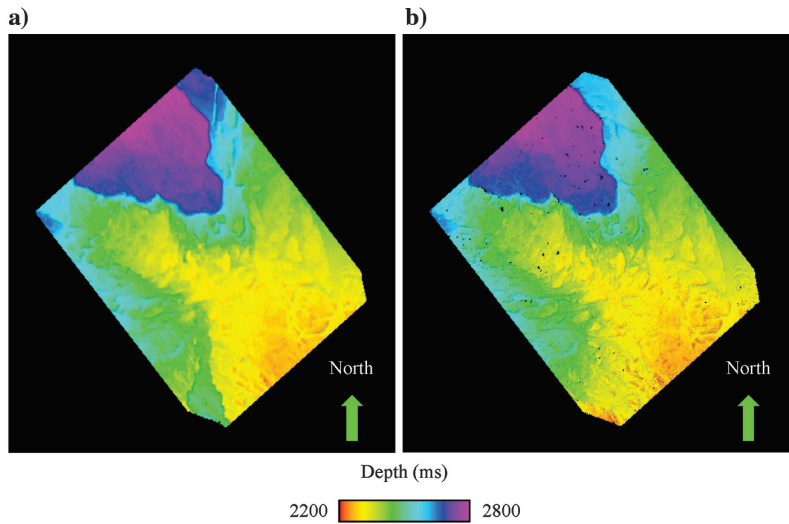
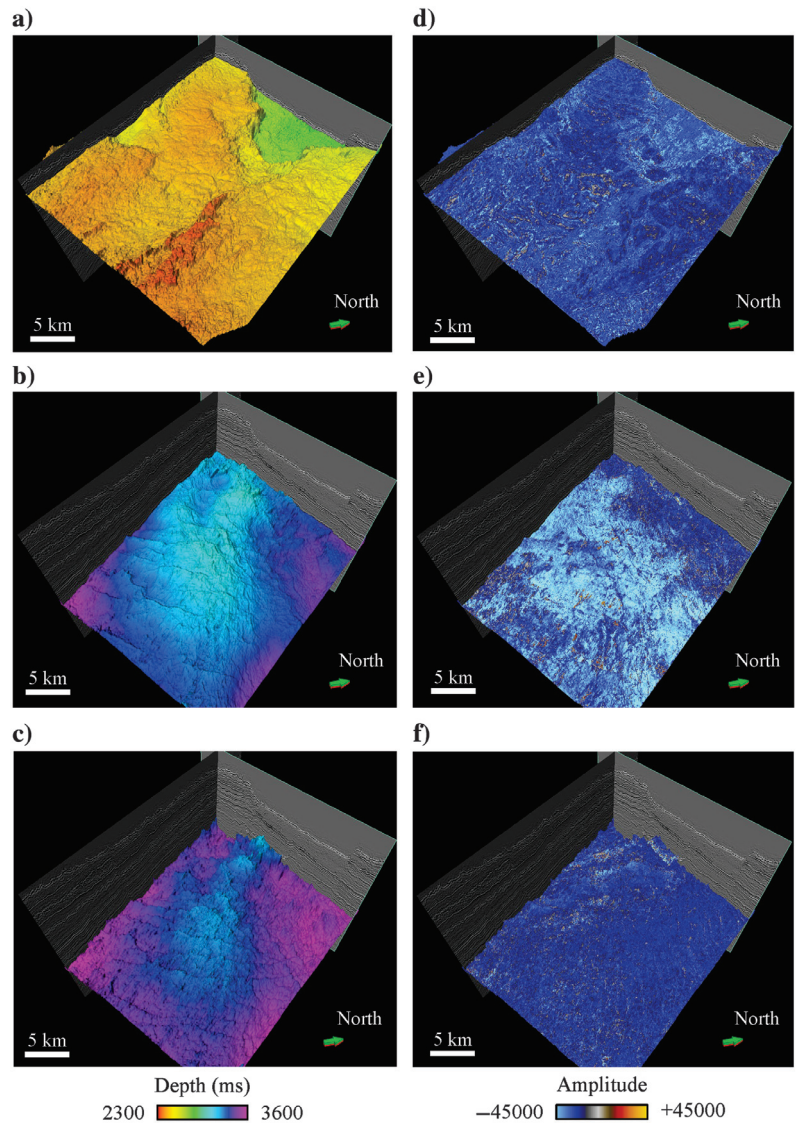


Figure 17. Comparison of the seafloor, the top horizon in the Solsikke data set extracted from (a) the proposed method, and (b) the conventional horizon tracker, colored by depth.



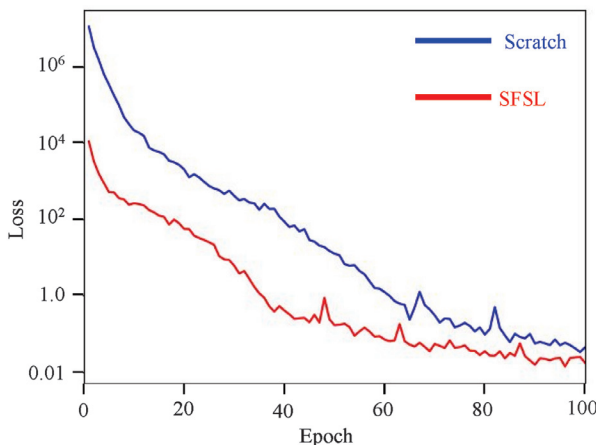


Figure 18. Comparison of the loss while training the SMB CNN from scratch (denoted by the blue curve) and the SFSL CNN (denoted by the red curve). Note the much lower initial loss and faster convergence by the SFSL-based training.

horizons by the conventional horizon tracker would require more and more time and effort from an interpreter. In such a case, the proposed method is able to help speed up the interpretation process while ensuring good interpretation accuracy.

### SFSL versus starting from scratch

As illustrated in Figure 1, one major innovation of the proposed workflow is to build the SMB CNN from the SFSL CNN instead of starting from scratch. For demonstrating the associated superiorities, we use the Solsikke seismic data set and build two SMB CNNs, one from the SFSL CNN and the other from scratch. Our observations are twofold. First, by inheriting the prior-known knowledge of understanding the target seismic signals from the SFSL CNN, the training of the SMB CNN starts with a lower loss and converges faster, as shown in Figure 18. Second, and more importantly, the use of the SFSL CNN grants the SMB CNN strong generalization ability and correspondingly improves the accuracy of stratigraphy interpretation at long distance because a seismic section typically becomes more distinct from the training sections with the distance between them increasing. However, because the SFSL CNN has already learned all of the seismic sections, the associated SMB CNN successfully inherits such knowledge and thereby is capable of making better prediction for the seismic sections at long distances. Figure 19 compares the prediction by both SMB CNNs in the IL2500 that is about 12 km (500 inlines) away from the training section. Even though both CNNs converge after training, as demonstrated by the loss curves in Figure 18, the SFSL-based prediction leads to significant improvement in delineating the sequences with much fewer misannotations.

### CONCLUSION

A semisupervised workflow has been presented for seismic stratigraphy interpretation by building two deep CNNs, one for SFSL and the other for SMB. Specifically, the SFSL CNN is unsupervised and is thereby capable of learning all of the seismic features in a given seismic data set by itself, whereas the SMB CNN is constructed from the SFSL network, so that it successfully inherits the prior-known knowledge about the seismic features in the target seis-

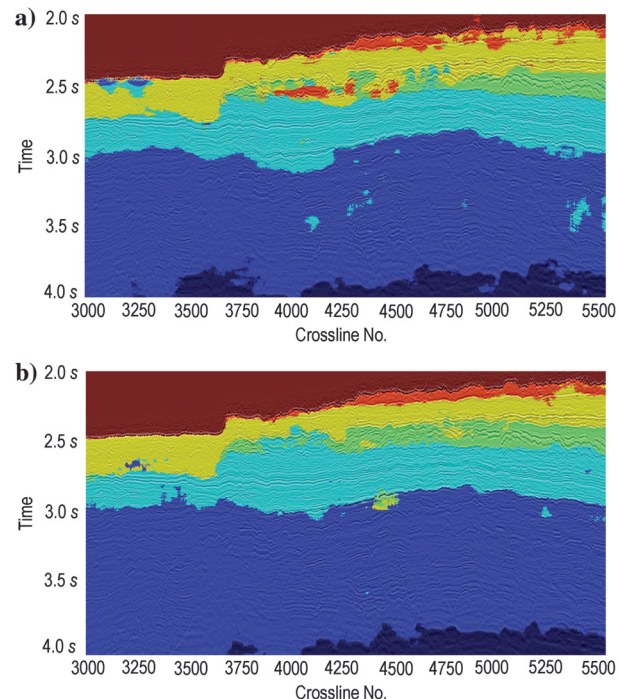


Figure 19. The comparison of the prediction in the section of inline 2500 that is about 12 km (500 inlines) away from the training section by the (a) SMB CNN trained from scratch and (b) the SFSL CNN. Apparently, even though both SMB CNNs converge well after training (Figure 18), the SFSL-based one leads to a significant improvement in the long-distance prediction with much fewer misannotations.

mic data set. Compared to the conventional approach of training an SMB CNN from scratch, the proposed workflow is superior in three aspects, including (1) a smaller amount of training data required, which is less than 0.08% of the available seismic data as tested in this work, (2) faster network training with a lower initial loss, and (3) stronger generalization ability for significantly improved stratigraphy interpretation at a long distance. Besides the demonstrated seismic stratigraphy interpretation, the SFSL is of great potential and can be readily applied for assisting with more challenges in seismic pattern recognition and interpretation, such as object detection and facies analysis. In addition, although the proposed workflow uses the seismic amplitude only for automated stratigraphy interpretation in this work, it can be readily extended for integration with more geologic fundamentals and/or rules, such as faults.

For the convenience of a seismic interpreter providing training data, the workflow is designed to be applicable in three application scenarios, including the trace-wise, paintbrushing, and full-sectional annotation. For example, the paintbrushing scenario allows the interpreter to provide annotation in any shape or orientation, which can help avoid interpreter bias in zones with interpretation uncertainties. The trace-wise scenario makes it possible for integrating seismic data and well logs, in which the most reliable information about the subsurface can be used for calibrating the seismic signals while making stratigraphy interpretation.

### ACKNOWLEDGMENT

Many thanks go to the assistant editor C. Torres-Verdin, the associate editor W. Li, and the reviewer X. Wu and one anonymous

reviewer for their insightful comments and suggestions on improving the quality of the paper. The neural network algorithm is developed and implemented using the open-source Python package *TensorFlow* developed by Google Brain.

## DATA AND MATERIALS AVAILABILITY

Data associated with this research are confidential and cannot be released.

## REFERENCES

- Agrawal, P., J. Carreira, and J. Malik, 2015, Learning to see by moving: IEEE International Conference on Computer Vision, 37–45.
- AlRegib, G., M. A. Deriche, Z. Long, H. Di, Z. Wang, Y. Alaudah, M. A. Shafiq, and M. Alfarraj, 2018, Subsurface structure analysis using computational interpretation and learning: IEEE Signal Processing Magazine, **35**, 82–98, doi: [10.1109/MSP.2017.2785979](https://doi.org/10.1109/MSP.2017.2785979).
- Araya-Polo, M., T. Dahlke, C. Frogner, C. Zhang, T. Poggio, and D. Hoh, 2017, Automated fault detection without seismic processing: The Leading Edge, **36**, 208–214, doi: [10.1190/tle36030208.1](https://doi.org/10.1190/tle36030208.1).
- Badrinarayanan, V., A. Kendall, and R. Cipolla, 2017, Segnet: A deep convolutional encoder-decoder architecture for image segmentation: IEEE Transactions on Pattern Analysis and Machine Intelligence, **39**, 2481–2495, doi: [10.1109/TPAMI.34](https://doi.org/10.1109/TPAMI.34).
- Di, H., and G. AlRegib, 2020, A comparison of seismic saltbody interpretation via neural networks at sample and pattern levels: Geophysical Prospecting, **68**, 521–535, doi: [10.1111/gpr.v68.2](https://doi.org/10.1111/gpr.v68.2).
- Di, H., D. Gao, and G. AlRegib, 2018a, 3D dip vector-guided auto-tracking for weak seismic reflections: A new tool for shale reservoir visualization and interpretation: Interpretation, **6**, no. 4, SN47–SN56, doi: [10.1190/INT-2018-0053.1](https://doi.org/10.1190/INT-2018-0053.1).
- Di, H., D. Gao, and G. AlRegib, 2019a, Developing a seismic texture analysis neural network for machine-aided seismic pattern recognition and classification: Geophysical Journal International, **218**, 1262–1275, doi: [10.1093/gji/gzj226](https://doi.org/10.1093/gji/gzj226).
- Di, H., Z. Li, H. Maniar, and A. Abubakar, 2019b, Seismic stratigraphy interpretation via deep convolutional neural networks: 89th Annual International Meeting, SEG, Expanded Abstracts, 2358–2362, doi: [10.1190/segam2019-3214745.1](https://doi.org/10.1190/segam2019-3214745.1).
- Di, H., C. Li, S. Smith, and A. Abubakar, 2019c, Machine learning-assisted seismic interpretation with geologic constraints: 89th Annual International Meeting, SEG, Expanded Abstracts, 5360–5364, doi: [10.1190/segam2019-w4-01.1](https://doi.org/10.1190/segam2019-w4-01.1).
- Di, H., Z. Wang, and G. AlRegib, 2018b, Seismic fault detection from post-stack amplitude by convolutional neural networks: 80th Annual International Conference and Exhibition, EAGE, Extended Abstracts, Tu-D-11.
- Di, H., Z. Wang, and G. AlRegib, 2018c, Deep convolutional neural networks for seismic salt-body delineation: AAPG Annual Convention and Exhibition.
- Dosovitskiy, A., P. Fischer, J. T. Springenberg, M. Riedmiller, and T. Brox, 2016, Discriminative unsupervised feature learning with exemplar convolutional neural networks: IEEE Transactions on Pattern Analysis and Machine Intelligence, **38**, 1734–1747, doi: [10.1109/TPAMI.2015.2496141](https://doi.org/10.1109/TPAMI.2015.2496141).
- Faraklouli, M., and M. Petrov, 2004, Horizon picking in 3D seismic data volumes: Machine Vision and Applications, **15**, 216–219, doi: [10.1007/s00138-004-0151-8](https://doi.org/10.1007/s00138-004-0151-8).
- Geng, Z., X. Wu, Y. Shi, and S. Fomel, 2019, Relative geologic time estimation using a deep convolutional neural network: 89th Annual International Meeting, SEG, Expanded Abstracts, 2238–2242, doi: [10.1190/segam2019-3214459.1](https://doi.org/10.1190/segam2019-3214459.1).
- Gidaris, S., P. Singh, and N. Komodakis, 2018, Unsupervised representation learning by predicting image rotations: Presented at the International Conference on Learning Representations.
- Gramstad, O., and J. Q. H. Bakke, 2012, Seismic surface extraction using iterative seismic DNA detection: 82nd Annual International Meeting, SEG, Expanded Abstracts, doi: [10.1190/segam2012-0600.1](https://doi.org/10.1190/segam2012-0600.1).
- Guitton, A., 2018, 3D convolutional neural networks for fault interpretation: Presented at the Annual Conference and Exhibition, EAGE.
- Harrigan, E., J. Kroh, W. Sandham, and T. Durrani, 1992, Seismic horizon picking using an artificial neural network: IEEE International Conference on Acoustics, Speech, and Signal Processing, 105–108.
- Herron, D. A., 2011, First steps in seismic interpretation: SEG, Geophysical Monograph Series No. 16.
- Herron, D. A., 2015, Pitfalls in horizon autopicking: Interpretation, **3**, no. 1, SB1–SB4, doi: [10.1190/INT-2014-0062.1](https://doi.org/10.1190/INT-2014-0062.1).
- Hoecker, C., and G. Fehmers, 2003, Fast structural interpretation with structure-oriented filtering: Geophysics, **68**, 238–243, doi: [10.1190/1.1598121](https://doi.org/10.1190/1.1598121).
- Huang, K. Y., 1997, Hopfield neural network for seismic horizon picking: 67th Annual International Meeting, SEG, Expanded Abstracts, 562–565, doi: [10.1190/1.1885963](https://doi.org/10.1190/1.1885963).
- Huang, L., X. Dong, and T. E. Clee, 2017, A scalable deep learning platform for identifying geologic features from seismic attributes: The Leading Edge, **36**, 249–256, doi: [10.1190/tle36030249.1](https://doi.org/10.1190/tle36030249.1).
- Kallenberg, M., K. Petersen, M. Nielsen, A. Ng, P. Diao, C. Igel, C. Vachon, K. Holland, R. Winkel, N. Karssemeijer, and M. Lillholm, 2016, Unsupervised deep learning applied to breast density segmentation and mammographic risk scoring: IEEE Transactions on Medical Imaging, **35**, 1322–1331, doi: [10.1109/TMI.2016.2532122](https://doi.org/10.1109/TMI.2016.2532122).
- Leggett, M., W. A. Sandham, and T. S. Durrani, 1996, 3-D Seismic horizon tracking using an artificial neural network: First Break, **14**, 413–418, doi: [10.3997/1365-2397.1996022](https://doi.org/10.3997/1365-2397.1996022).
- Li, Z., H. Di, H. Maniar, and A. Abubakar, 2019, Semi-supervised deep machine learning assisted seismic image segmentation and stratigraphic sequence interpretation: 81st Annual International Conference & Exhibition, EAGE, Extended Abstracts, Th\_P04\_04.
- Long, J., E. Shelhamer, and T. Darrell, 2015, Fully convolutional networks for semantic segmentation: IEEE Conference on CVPR.
- Noh, H., S. Hong, and B. Han, 2015, Learning deconvolution network for semantic segmentation: IEEE International Conference on Computer Vision.
- Patel, D., S. Bruckner, I. Viola, and M. E. Groller, 2010, Seismic volume visualization for horizon extraction: Pacific Visualization Symposium, IEEE, Extended Abstracts, 73–80.
- Peters, B., J. Granek, and E. Haber, 2019, Multi-resolution neural networks for tracking seismic horizons from few training images: Interpretation, **7**, no. 3, SE201–SE213, doi: [10.1190/INT-2018-0225.1](https://doi.org/10.1190/INT-2018-0225.1).
- Ronneberger, O., P. Fischer, and T. Brox, 2015, U-net: Convolutional networks for biomedical image segmentation: International Conference on Medical Image Computing and Computer-assisted Intervention, 234–241.
- Wang, Z., H. Di, M. A. Shafiq, Y. Alaudah, and G. AlRegib, 2018, Successful leveraging of image processing and machine learning in seismic structural interpretation: A review: The Leading Edge, **37**, 451–461, doi: [10.1190/tle37060451.1](https://doi.org/10.1190/tle37060451.1).
- Wu, X., and D. Hale, 2015, Horizon volumes with interpreted constraints: Geophysics, **80**, no. 2, IM21–IM33, doi: [10.1190/geo2014-0212.1](https://doi.org/10.1190/geo2014-0212.1).
- Wu, X., L. Liang, Y. Shi, and S. Fomel, 2019a, FaultSeg3D: Using synthetic datasets to train an end-to-end convolutional neural network for 3D seismic fault segmentation: Geophysics, **84**, no. 3, IM35–IM45, doi: [10.1190/geo2018-0646.1](https://doi.org/10.1190/geo2018-0646.1).
- Wu, H., B. Zhang, T. Lin, D. Cao, and Y. Lou, 2019b, Semiautomated seismic horizon interpretation using the encoder-decoder convolutional neural network: Geophysics, **84**, no. 6, B403–B417, doi: [10.1190/geo2018-0672.1](https://doi.org/10.1190/geo2018-0672.1).
- Xiong, W., X. Ji, Y. Ma, Y. Wang, N. M. AlBinHassan, M. N. Ali, and Y. Luo, 2018, Seismic fault detection with convolutional neural network: Geophysics, **83**, no. 5, O97–O103, doi: [10.1190/geo2017-0666.1](https://doi.org/10.1190/geo2017-0666.1).
- Yu, Y., C. Kelley, and I. Mardanova, 2008, Seismic horizon autopicking using orientation vector field: U.S. Patent 8,265,876.
- Yu, Y., C. Kelley, and I. Mardanova, 2011, Automatic horizon picking in 3D seismic data using optical filters and minimum spanning tree (patent pending): 81st Annual International Meeting, SEG, Expanded Abstracts, 965–969, doi: [10.1190/1.3628233](https://doi.org/10.1190/1.3628233).
- Zeiler, M., G. Taylor, and R. Fergus, 2011, Adaptive deconvolutional networks for mid and high level feature learning: Presented at the International Conference on Computer Vision.
- Zhao, T., and P. Mukhopadhyay, 2018, A fault-detection workflow using deep learning and image processing: SEG Technical Program, Expanded Abstracts, 1966–1970, doi: [10.1190/segam2018-2997005.1](https://doi.org/10.1190/segam2018-2997005.1).